AUT Journal of Modeling and Simulation

AUT J. Model. Simul., 56(1) (2024) 3-18
DOI: 10.22060/miscj. 2024.23304.5364

# Decentralized Optimization in the Scheduling of Three Virtual Power Plants with Non-Convex Constraints

Amir Hossein Gholami [1]*, Amir Abolfazl Suratgar[1], Mohammad Bagher Menhaj [1], Mohammad Reza Hesamzadeh [2]

[1] Distributed Intelligent Optimization Research Laboratory, Department of Electrical Engineering, Amirkabir University, Tehran, Iran
[2] Department of Electrical Engineering and Computer Science, KTH, Stockholm, Sweden

**ABSTRACT:** Virtual power plant planning (VPP) has received much attention in recent years. VPP refers to the integration of multiple power units, considered as a single power plant. In this paper, three VPPs are considered, each consisting of different power plant units and expected to supply the desired load. In addition to providing the desired load, they must maximize their profits. A decentralized optimization method was used to optimize these three VPPs. The reason for using a decentralized approach is to increase network security and eliminate the need for a central computer. However, using decentralized optimization increases the speed of problem-solving. Finally, the obtained results are compared with the centralized method. Simulations show that almost the same results are achieved using different optimization methods. These results increase the trend of using decentralized methods in VPP. Another feature of decentralized methods compared to the centralized method is the reduction in the speed of problem-solving, which in this article has greatly reduced the solution time. If the considered network becomes wider and the number of problem variables and their limitations increases, the use of decentralized methods will become more efficient, and in those problems, the difference in problem-solving time by centralized and decentralized methods will increase.

**Review History:**

Received: Jun. 25, 2024
Revised: Aug. 01, 2024
Accepted: Aug. 09, 2024
Available Online: Sep. 05, 2024

**Keywords:**

Decentralized Optimization
Virtual Power Plant (VPP)
ADMM Algorithm
Fast ADMM Algorithm
Fast ADMM with Restart Algorithm

## 1- Introduction

Nowadays, due to many reasons such as technological advancement, population growth, geographical expansion, etc., the thought of a network of power plants to provide the required amount of electricity to the people has increased significantly [1, 2]. Virtual power plant (VPP) optimization is one of the topics that has received a lot of attention in the last decade and planning for them is very important. Virtual power plant refers to the integration of several different power plant units, called a single power plant. A lot of research has been done on virtual power plant planning; some of the most recent studies are presented below.

Reference [3] discusses VPP scheduling. Their main objective is to minimize costs and emissions. They used a centralized approach to solve their optimization problem. Solar, wind, combined heat and power units, power-to-gas technology and carbon sorption power plants have been used. One of the disadvantages of this research is that only one VPP is used in the problem and they do not pay attention to the network of VPPs. Reference [4] addresses the problem of maximum profit allocation to power plant units based on multi-objective optimization. Their other goals include equitable profit distribution among power plant units, stable cooperation between units, and attracting power plant units to expand VPP. Decentralized optimization methods have not been taken into account in this reference. The performance of virtual power plants with shared storage has been studied in reference [5]. Emergency-shared energy storage provides a solution for the use of renewable energy sources. In this research, four virtual power plants with the same model were used, which helps to solve the optimization problem in a centralized way. Its main objective is to achieve maximum profits in different power plant units.

Many other researches have all used a centralized approach to optimize their VPP. References [6-14] use the centralized method. On the other hand, references [15-33] have also done very similar work. In this paper, the goal is to use a decentralized optimization method in the VPP network. The innovations in this article are:

Consider three VPPs with different units.

Use of the decentralized optimization method and comparison of some of its algorithms with each other

Comparison of simulations performed with the centralized method along with analysis

The considered grid consisting of three VPPs is shown in Fig. 1.

According to Fig. 1, wind turbine (WT), photovoltaic (PV), combined heat and power (CHP), pumped hydro storage (PHS), battery energy storage system (BESS) and diesel generator (DG) were used. In the second part of this article, different power plant units will be considered. In the third part, the algorithms used for simulation will be briefly

*Corresponding author's email: amirhoseingholami75@ gmail.com

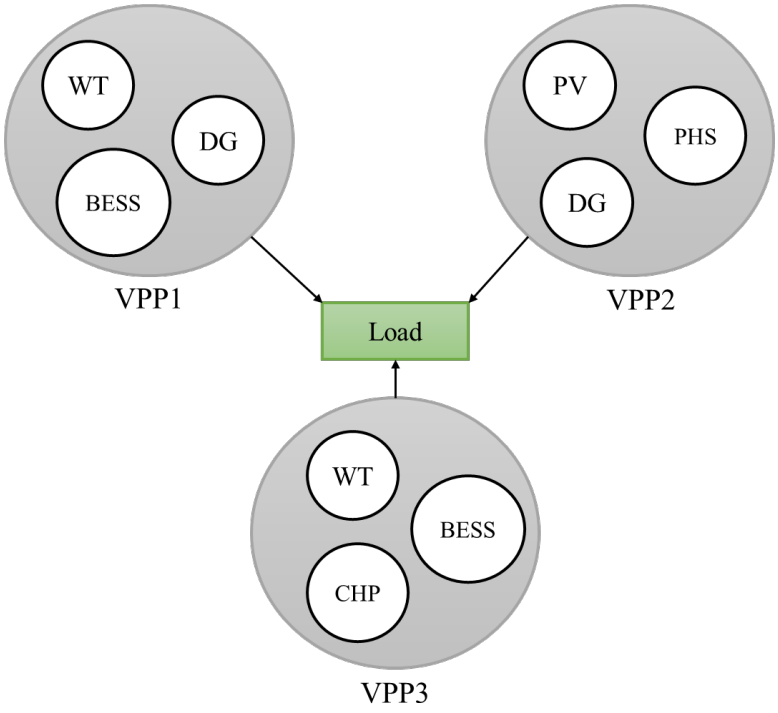


**Fig. 1. A view of the desired grid.**

reviewed. In the fourth section, the desired model and its necessary mathematical equations are presented. In the fifth part, the simulation results are analyzed. In the sixth part, a conclusion is also given.

## 2- Power Plant Units and Their Mathematical Models

In this part of the article, the goal is to consider models of different power plant units; the model of each unit is selected from a reference. Photovoltaics and wind turbines are considered very important renewable units that are receiving a lot of attention today. Solar cells generate electrical energy based on the amount of sunlight hitting the panel, the ambient temperature, and its manufacturing specifications. There are many different static models of photovoltaic cells; the following model [34] is used :

$$T_{cell}(t) = T_{amp}(t) + SR(t) \times \left(\frac{NOT_{cell}-20}{0.8}\right) \quad (1)$$

$$I(t) = SR(t) \times [I_{scc} + K_{ctc} \times (T_{cell}(t) - 25)] \quad (2)$$

$$V(t) = V_{ocv} - K_{vtc} \times T_{cell}(t) \quad (3)$$

$$FL = \frac{V_{max} \times I_{max}}{V_{ocv} \times I_{scc}} \quad (4)$$

$$P_{PV}(t) = FL \times V(t) \times I(t) \quad (5)$$

That $T_{cell}$ is solar cell temperature ($^{\circ}C$), $T_{amp}$ is ambient temperature ($^{\circ}C$), $SR$ is solar radiation ($kw/m^2$), $NOT_{cell}$ is cell Solar cell nominal operating temperature ($^{\circ}C$), $I$ is solar cell output current (A), $I_{scc}$ is solar cell short circuit current (A), $K_{ctc}$ is temperature coefficient Solar cell current (A/$^{\circ}C$), $V$ is Solar cell output voltage (V), $V_{ocv}$ is Solar cell open circuit voltage (V), $K_{vtc}$ is Solar cell voltage temperature coefficient (V/$^{\circ}C$), $V_{max}$ is solar cell voltage at maximum power point (V), $I_{max}$ is solar cell current at maximum power point (A), FL is solar cell charge coefficient and $P_{PV}$ is solar cell output power (MW).

Additionally, wind turbines generate power based on the speed at which the wind hits their blades. Normally, in order not to damage the wind turbine when the wind speed is too high, if the wind speed exceeds a certain limit, the wind turbine will not produce electricity. There are many different models for this power plant unit; the model presented in [16] is used:

$$P_{WT}(t)=\begin{cases}0 & v(t)<v_{in}\\ P_{rtd}^{wt}\times\left(\frac{v(t)-v_{in}}{v_{rtd}-v_{in}}\right)^3 & v_{in}\le v(t)\le v_{rtd}\\ P_{rtd}^{wt} & v_{rtd}\le v(t)<v_{out}\\ 0 & v_{out}\le v(t)\end{cases} \quad (6)$$

Where $P_{WT}$ is wind turbine output power (MW), $P_{rtd}^{wt}$ is nominal wind turbine power (MW), $v$ is wind speed (m⁄sec), $v_{in}$ is the cut-in speed in a wind turbine (m⁄sec), $v_{out}$ is the cut-out speed in a wind turbine (m⁄sec) and $v_{rtd}$ is the rated speed of a wind turbine (m⁄sec).

Combined heat and power (CHP) plant is another widely used power generation unit that produces electrical and thermal energy at the same time. This powerhouse usually produces a lot of power and can power large loads, but one of its disadvantages is the creation of pollutants in the environment. There are also different models for this energy production unit, among which the model [34] is used.

Diesel generators (DGs) are another device used in emergencies. The power that this power plant can generate is between the low and high ranges, expressed by equation (7).

$$P_{dg}^{min}\le P_{dg}(t)\le P_{dg}^{max} \quad (7)$$

In other words, $P_{dg}(t)$ is the power generated by the DG in one hour (MW). The energy storage system is also another unit used in the problem. These systems come in many different types, the most important of which are BESS and PHS. BESS is a widely used system today. Because this system has a relatively high cost, to increase lifespan, people consider the energy reserve from 10% to 90% so that the battery has a longer life. The battery power equation, which is a dynamic equation, is derived from the following equation:

$$E(t+1)=E(t)+\eta_{ch}.P_{ch}(t)-\frac{P_{dis}(t)}{\eta_{dis}} \quad (8)$$

E is the battery energy in the BESS (MWh), $\eta_{ch}$ is the battery charging efficiency (%) and $\eta_{dis}$ is the battery discharge efficiency (%). Based on equation (8), the battery's energy per hour depends on the charging and discharging capacity of the battery and the battery's energy in the previous hours. Pumped hydro storage (PHS) units are often established near the sea and have reservoirs at water levels above the sea. When the electricity produced is greater than the electricity consumed, seawater is pumped back to the reservoir for storage. On the other hand, if electricity is needed, water is transferred from the reservoir to the sea and electricity is produced. The volume of the upper reservoir in the PHS system is dynamic and is calculated from the following equation:

$$P_{ch}(t).P_{dis}(t)=0 \quad (9)$$

$$P_p(t).P_T(t)=0 \quad (10)$$

This means $P_{ch}$ charges (MW) and $P_{dis}$ discharges (MW) in the BESS system. Furthermore, $P_p$ is the power consumed from the sea to the upper reservoir of the PHS (MW) and $P_T$ is the electricity produced from the reservoir to the sea in the (MW) PHS system. The rest of the BESS system equations are selected from reference [34] and the PHS system equations from reference [35]. The reason for using the above equations in these systems is that they cannot produce and consume energy at the same time. As can be seen from equations (9) and (10), these constraints lead to the non-convexity of the problem constraints, and as a result, the overall optimization problem will be a non-convex nonlinear optimization problem. So, in this section, the models of different units have been considered. In the following section, a brief introduction to different algorithms will be given.

## 3- Decentralized Optimization Algorithms

In this part of the article, the aim is to briefly review the algorithms used in the simulation. The decentralized algorithms used in the simulation are ADMM, Fast ADMM, and Fast ADMM with restart. The Alternating Direction Method of Multipliers (ADMM) algorithm is one of the decentralized optimization methods. ADMM algorithm has proof of convergence and is one of the most used algorithms. To present this algorithm more precisely, consider the following optimization problem:

$$\min_{x,y} f(x)+g(y) \quad (11)$$

$$s.t.\ Ax+By=C \quad (12)$$

In this optimization problem, x and y are the decision variables. A, B and C are the matrices (vectors) of the coefficients of the equality constraint. Now, to obtain the decision variables using the ADMM algorithm, the Lagrange function must be written, and the result is:

$$L(x,y,\lambda)=f(x)+g(y)$$
$$+\lambda^T(Ax+By-C)+\frac{\rho}{2}\|Ax+By-C\|_2^2 \quad (13)$$

In this equation, λ is the Lagrange multiplier and ρ is a positive coefficient. Now the decision variables and Lagrange coefficients are obtained from the following equation:

$$x(k+1) = \arg\min_{x} L\big(x, y(k), \lambda(k)\big) \quad (14)$$

$$y(k+1) = \arg\min_{y} L\big(x(k+1), y, \lambda(k)\big) \quad (15)$$

$$\lambda(k+1) = \lambda(k) + \rho(Ax + By - C) \quad (16)$$

Therefore, the initial conditions for y and λ are determined first, and the decision variables are calculated according to the above equations. Additional details are available in reference [36] for ADMM algorithm. If there are inequality constraints in the optimization problem, they should be added to the Lagrange function and Karush-Kuhn-Tucker (KKT) conditions should be used to obtain them.

Fast ADMM and Fast ADMM with Restart Algorithm are additional versions of the standard ADMM algorithm that make minor changes to the equations and can be reviewed in Reference [36, 37]. The Fast ADMM and Fast ADMM with Restart versions are designed to increase the speed of the standard ADMM algorithm itself. These three algorithms (ADMM, Fast ADMM, Fast ADMM with restart) are implemented on the optimization problem and their simulation results are compared with the centralized method. In the following section, the optimization problem will be studied in detail.

## 4- Optimization Problem and Constraints

In this article, the objective is to minimize the cost (maximize profit) of power plant units. The nine power plant units are distributed into three VPPs, which must be able to ensure the balance of electrical and thermal energy and, on the other hand, minimize costs. The cost function of this optimization problem is written as the following equation.

$$\min_{P_{units}(t)} Cost =$$

$$\sum_{t=1}^{24}(C_{DG1}(t) + C_{BESS1}(t) + C_{PHS2}(t) \quad (17)$$

$$+C_{DG2}(t) + C_{CHP3}(t) + C_{BESS3}(t))$$

In equation (18), the costs of power plant units are stated, each of which has a mathematical equation and is displayed as follows:

$$C_{DG1}(t) = N_{DG1}.\pi_{DG1}.P_{DG1}(t) \quad (18)$$

$$C_{BESS1}(t) = N_{BESS1}.\pi_{BESS1}.\big(P_{ch1}(t) + P_{dis1}(t)\big) \quad (19)$$

$$C_{PHS2}(t) = N_{PHS2}.\pi_{PHS2}.\big(P_{P2}(t) + P_{T2}(t)\big) \quad (20)$$

$$C_{DG2}(t) = N_{DG2}.\pi_{DG2}.P_{DG2}(t) \quad (21)$$

$$C_{CHP3}(t) = N_{CHP3}.\pi_{CHP3}.P_{CHP3}(t) \quad (22)$$

$$C_{BESS3}(t) = N_{BESS3}.\pi_{BESS3}.\big(P_{ch3}(t) + P_{dis3}(t)\big) \quad (23)$$

The equation from (18) to (23) shows the cost of electricity production at each unit of power plant. $N_{unit}$ indicates the number of each power plant unit. $\pi_{unit}$ also represents the hourly electricity production factor ($/MW). $P_{unit}$ represents the generating capacity of each power plant unit (MW). Power balance limits are also shown below.

$$N_{DG1}.P_{DG1}(t) + N_{BESS1}.\big(P_{dis1}(t) - P_{ch1}(t)\big)$$

$$+N_{PHS2}.\big(P_{T2}(t) - P_{P2}(t)\big) + N_{DG2}.P_{DG2}(t) \quad (24)$$

$$+ N_{CHP3}.P_{CHP3}(t) + N_{BESS3}.\big(P_{dis3}(t) - P_{ch3}(t)\big) = \hat{P}_L(t)$$

$$\hat{P}_L(t) = P_L(t) - N_{WT1}.P_{WT1}(t)$$

$$-N_{PV2}.P_{PV2}(t) - N_{WT3}.P_{WT3}(t) \quad (25)$$

$$N_{CHP3}.H_{chp3}(t) = H_L(t) \quad (26)$$

In other words, $H_{chp3}$ is the thermal energy generated CHP and $H_L$ is the thermal energy of the load. In addition to the power balance constraint in the network, each power plant unit also has constraints that need to be added to the problem and solved based on the presented algorithms. Now it is necessary to determine the parameters used for simulation in the units of the power plant, which are indicated in the following tables.

In the result, these values are used to simulate the presented decentralized algorithm. The simulation results will be discussed in the next section.

Simulation and Results

In this part, the optimization problem is simulated.

**Table 1. Number of different power plant units**

| Parameters | Value |
|---|---|
| $N_{DG1}$ | 1 |
| $N_{DG2}$ | 1 |
| $N_{BESS1}$ | 2 |
| $N_{BESS3}$ | 5 |
| $N_{PHS2}$ | 3 |
| $N_{CHP3}$ | 5 |
| $N_{WT1}$ | 1 |
| $N_{WT3}$ | 5 |
| $N_{PV2}$ | 50 |

**Table 2. DG unit parameters [38]**

| Parameters | Name | Value |
|---|---|---|
| $P_{dg1}^{min}$ | Minimum power in DG (MW) | 0.0012 |
| $P_{dg1}^{max}$ | Maximum power in DG (MW) | 0.003 |
| $P_{dg2}^{min}$ | Minimum power in DG (MW) | 0.002 |
| $P_{dg2}^{max}$ | Maximum power in DG (MW) | 0.005 |

**Table 3. Power generation cost coefficients per power plant unit [38, 39]**

| Parameters | Value |
|---|---|
| $\pi_{DG1}$ $(\$/MW)$ | 0.01 |
| $\pi_{DG2}$ $(\$/MW)$ | 0.02 |
| $\pi_{BESS1}$ $(\$/MW)$ | 0.03 |
| $\pi_{BESS3}$ $(\$/MW)$ | 0.04 |
| $\pi_{PHS2}$ $(\$/MW)$ | 0.01 |
| $\pi_{CHP3}$ $(\$/MW)$ | 0.005 |

**Table 4. PV unit parameters [34]**

| Parameters | Name | Value |
|---|---|---|
| $I_{scc}$ | Short circuit current (A) | 5.32 |
| $I_{max}$ | Maximum current (A) | 4.76 |
| $V_{ocv}$ | Open circuit voltage (V) | 21.98 |
| $V_{max}$ | Maximum voltage (V) | 17.32 |
| $K_{ctc}$ | Current coefficient | 0.0012 |
| $K_{vtc}$ | Voltage coefficient | 0.001 |
| $NOT_{cell}$ | Nominal current of the solar cell (℃) | 43 |

**Table 5. WT unit parameters [34]**

| Parameters | Name | Value |
|---|---|---|
| $v_{cut-in}$ | Cut-in speed (m/sec) | 2.5 |
| $v_{cut-out}$ | Cut-out speed (m/sec) | 28 |
| $v_{nom}$ | Nominal speed (m/sec) | 12 |
| $P_{WT-nom}$ | Nominal power in wind turbine (MW) | 1.8 |

**Table 6. PHS unit parameters [35]**

| Parameters | Name | Value |
|---|---|---|
| $P_{T2}^{min}$ | Low band in generator power (MW) | 0 |
| $P_{T2}^{max}$ | Upper band in generator power (MW) | 50 |
| $P_{P2}^{min}$ | Low band in pump power (MW) | 0 |
| $P_{P2}^{max}$ | Upper band in pump power (MW) | 55 |
| $\eta_T$ | Generator efficiency (%) | 95 |
| $\eta_P$ | Pump efficiency (%) | 90 |
| $\eta_{WP}$ | Efficiency of pipelines (%) | 98 |
| $\rho$ | Water density (Kg/m$^3$) | 1000 |
| $h$ | Tank height (m) | 60 |
| $W_{min2}$ | The lower band of the water volume inside the tank (m$^3$) | 10000 |
| $W_{max2}$ | The upper band of the water volume inside the tank (m$^3$) | 50000 |

**Table 7. BESS unit parameters [15, 34]**

| Parameters | Name | Value |
|---|---|---|
| $E_1^{min}$ | Minimum battery energy (MWh) | 0.141 |
| $E_1^{max}$ | Maximum battery energy (MWh) | 1.273 |
| $E_3^{min}$ | Minimum battery energy (MWh) | 0.3 |
| $E_3^{max}$ | Maximum battery energy (MWh) | 1.5 |
| $P_{ch1}^{max}$ | Maximum battery charging power (MW) | 0.283 |
| $P_{dis1}^{max}$ | Maximum battery discharging power (MW) | 0.283 |
| $P_{ch3}^{max}$ | Maximum battery charging power (MW) | 0.2 |
| $P_{dis3}^{max}$ | Maximum battery discharging power (MW) | 0.2 |
| $\eta_{ch1}$ | Battery charging efficiency (%) | 91.4 |
| $\eta_{dis1}$ | Battery discharging efficiency (%) | 91.4 |
| $\eta_{ch3}$ | Battery charging efficiency (%) | 90 |
| $\eta_{dis3}$ | Battery discharging efficiency (%) | 90 |

**Table 8. CHP unit parameters [39]**

| Parameters | Name | Value |
|---|---|---|
| $P_{CHP}^{A}$ | CHP electrical power at point A (MW) | 247 |
| $P_{CHP}^{B}$ | CHP electrical power at point B (MW) | 215 |
| $P_{CHP}^{C}$ | CHP electrical power at point C (MW) | 81 |
| $P_{CHP}^{D}$ | CHP electrical power at point D (MW) | 98 |
| $H_{CHP}^{A}$ | CHP heat power at point A (MWth) | 0 |
| $H_{CHP}^{B}$ | CHP heat power at point B (MWth) | 180 |
| $H_{CHP}^{C}$ | CHP heat power at point C (MWth) | 81 |
| $H_{CHP}^{D}$ | CHP heat power at point D (MWth) | 0 |

The constrained optimization problem with decentralized algorithms (ADMM, fast ADMM, and fast ADMM with restart) is simulated and compared. Fig. 2 shows the objective function of this optimization problem in different iterations, solved in a decentralized manner. Furthermore, in this figure, the results are compared with the optimal value obtained from the centralized method.

As shown in Fig. 2, the value of the objective function in the three decentralized methods and the results obtained with the centralized method are almost the same. This shows that it is possible to solve VPP optimization problems using a decentralized approach and achieve exact solutions for them. The value of the cost function based on the centralized method is 62.8 USD, while the value of the cost function in the decentralized methods is 62.6 USD, meaning the gap between the centralized and decentralized methods Concentration is almost zero. It is now necessary to verify that a balance of thermal and electrical energy has been established in the network that Figures 3 and 4 reflect these issues.

All decision variables in the optimization problem also

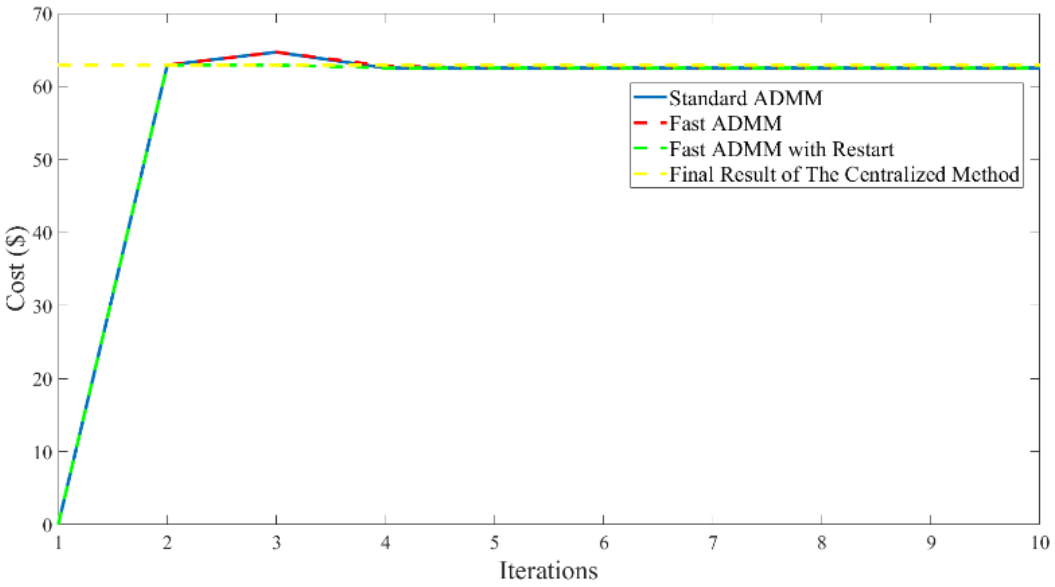


**Fig. 2. Objective function in different iterations.**

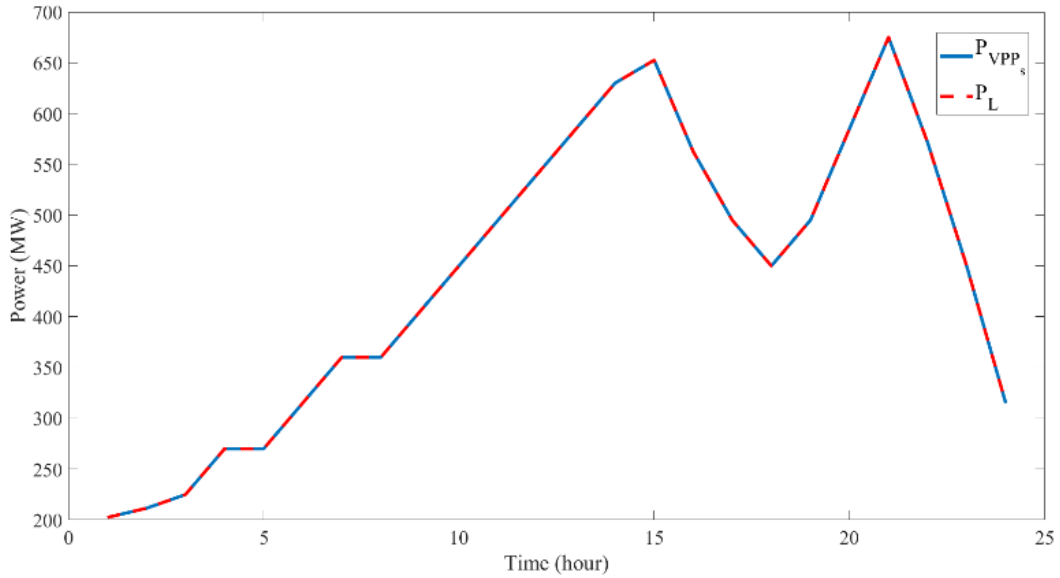


**Fig. 3. Electric power balance in the grid.**

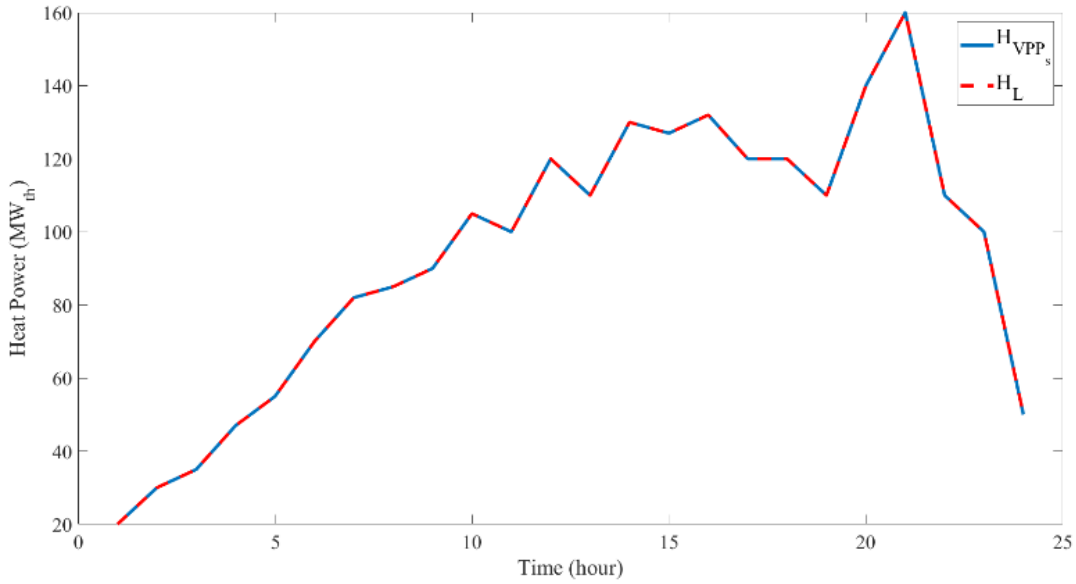


**Fig. 4. Heat power balance in the grid.**

satisfy the constraints and the optimization problem has been solved correctly. Based on Figures 3 and 4, it can be seen that over 24 hours, the balance of power was well established and the algorithms performed well.

The simulation is performed for $\rho = 10^7$. One of the most important parameters of the ADMM algorithm and its various versions is the correct choice of $\rho$. It is now necessary to examine the impact of changes in this parameter on the objective function. Fig. 5 shows the impact of these changes on the objective function for seven different ρ, solved using the standard ADMM algorithm. Based on Fig. 5, it can be seen that if a suitable number for $\rho$ is considered, the cost function will reach its optimal value in the minimum number of repetitions. If the value of the parameter $\rho$ exceeds a certain limit, the response may be inclined to a non-optimal value and may even diverge. Therefore, according to the coefficients in the objective function, the value of $\rho$ should be selected with a suitable ratio and reach the optimal value.

Now, the most important issue that must be investigated in this section is the production of power in different power plant units, and whether all power plant units have been able to meet their limitations or not. Fig. 5 shows the output power of each power plant unit using the ADMM algorithm in full.

As it is clear from Fig. 5, there are nine units in the target network, whose power generation is displayed in different subplots. As it is clear from these figures, all the units have met their limits correctly, the optimization problem has been correctly solved, and the obtained valuesare optimal.

Based on Fig. 5, subplot (a) shows the power generation of the diesel generator in the first VPP, which initially has a value between the minimum and maximum bands and after a while, it reaches its maximum value. Also, subplot (b) is related to the charging and discharging of the BESS system in the first VPP, which, considering that the initial conditions in the battery are considered, the charging power was at 24 zero, but a small amount of power was discharged from this system to the power grid. Another system used in the first VPP is the wind turbine, whose output power is shown in subplot (c). According to the model shown in equation (6), if the wind speed is less than a certain limit, the production power will be zero, and if the wind speed is too high, the power will be reduced due to the prevention of damage to the turbine blades and related equipment. Will be zero and otherwise it will produce power based on this equation.

Based on subplots (d), (h) and (i) in the second and third VPPs, a similar performance has occurred for power plant units. Another unit considered in the network and located in the second VPP is the PHS system, whose production power is shown in subplot (e). Based on the initial conditions considered for this unit and the considered optimization problem, a small amount of water was transferred from the top to the bottom of the tank and the generator of this system was activated and produced electric power, but the pump of this system had no activity. One of the renewable power plant units used in the second VPP and shown in subplot (f) is PVs. Due to the fact that there is no sunlight in some hours, this power plant unit cannot produce power, and in the rest of the day, it will produce power based on the amount of sunlight, based on which the power is obtained in this way. The last power plants in this network are CHPs, five CHP units have been used in the third VPP, which have been able to produce significant power. The noteworthy point in this network is the

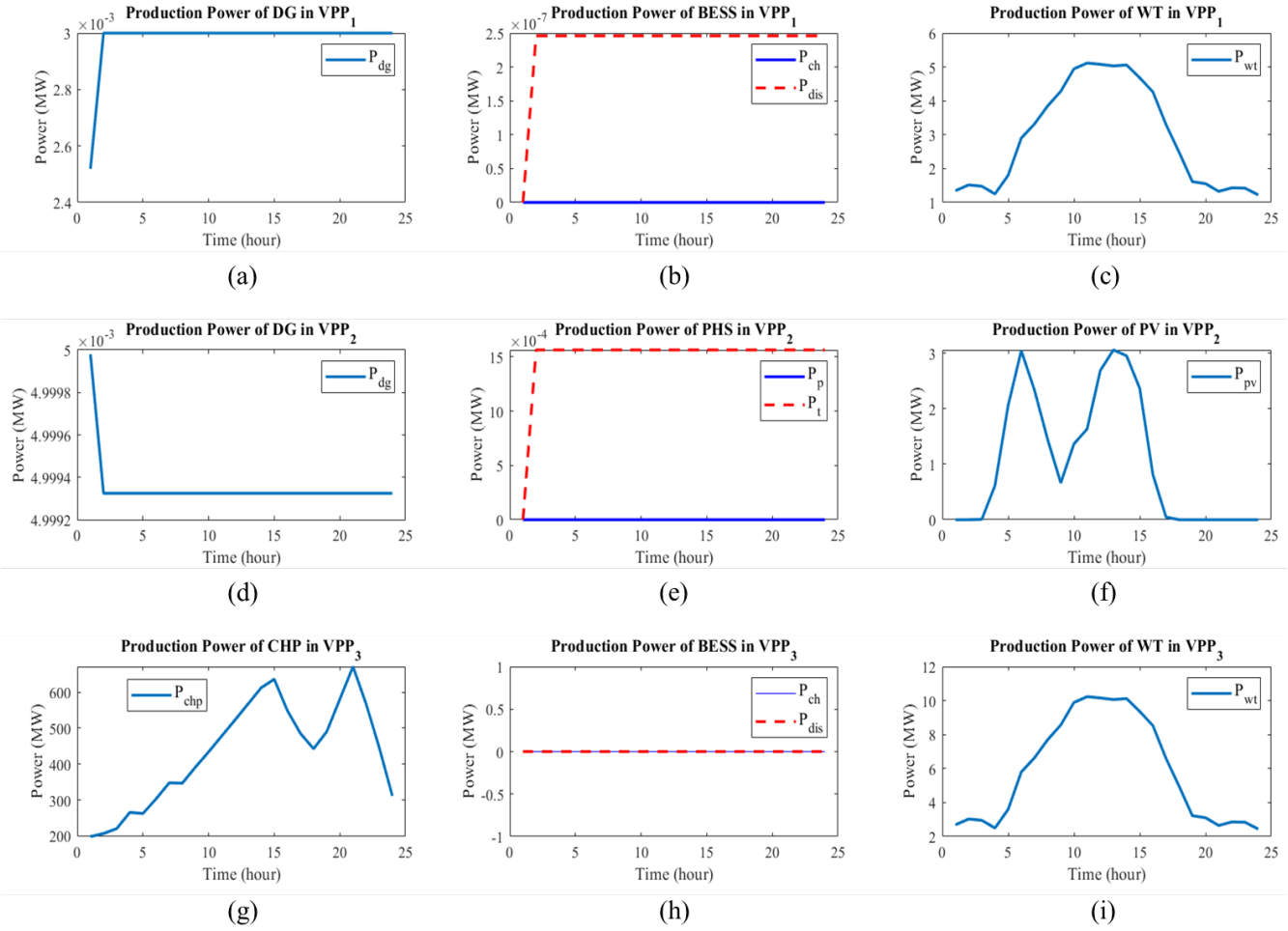


**Fig. 5. The power produced by different power plant units in the network (MW). (a) Production power of DG in VPP1, (b) Production power of BEES in VPP1, (c) Production power of WT in VPP1, (d) Production power of DG in VPP2, (e) Production power of PHS in VPP2, (f) Production power of PV in VPP2, (g) Production power of CHP in VPP3, (h) Production power of BESS in VPP3, (i) Production power of WT in VPP3.**

energy storage systems, namely BESS and PHS, which have not performed, and this is logical because energy storage systems enter the network if the generated power is more than the consumed power or the consumed power is more than the generated power. If the production and consumption power are equal, there is no need to enter energy storage systems into the grid, and subplots (b), (e) and (h) express exactly the same issue. In general, if the power required by the load increases and the power plant units cannot provide it, the energy storage systems will enter the network to supply the load power and transfer more power to the network.

Next, three scenarios for this network will be examined. In the first scenario, from 10:00 to 15:00 in the third VPP, a technical problem occurs for the wind turbines and they go out of the network, and after solving the problem, they return to the network from 15:00. Fig. 6 shows a view of the production power of different power plant units in this state.

As shown in Figure 6, wind turbines have been disconnected from the network from 10 to 15 hours, and this figure shows the production power of all the units in the network. Based on this, because the power produced by the wind turbines in the third VPP has been fully supported by the CHPs with their high capacity, so the CHPs have compensated for it and in total loads have been supplied. The noteworthy point is that the performance of other power plant units has not changed much and CHPs have supplied the main load of the network. But it is necessary to carefully examine why CHP units have only done this, the reason is that according to Table 3, the cost

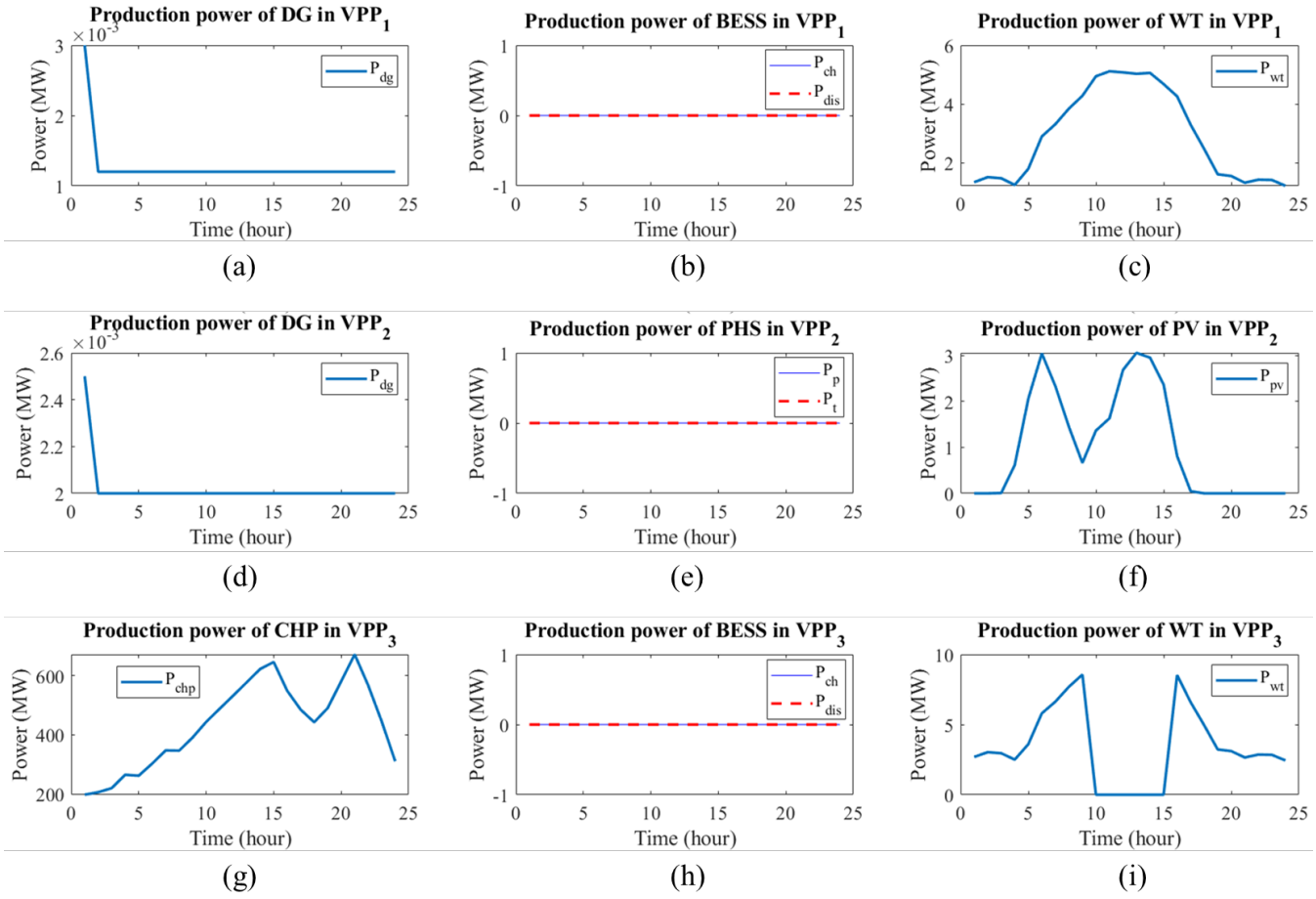


**Fig. 6. The power produced by different power plant units in the network (MW) in the scenario one. (a) Production power of DG in VPP1, (b) Production power of BEES in VPP1, (c) Production power of WT in VPP1, (d) Production power of DG in VPP2, (e) Production power of PHS in VPP2, (f) Production power of PV in VPP2, (g) Production power of CHP in VPP3, (h) Production power of BESS in VPP3, (i) Production power of WT in VPP3.**

of generating power in CHP is lower than other power plant units, and to minimize the cost, it is reasonable to Only use the capacity of these power plants. The number of CHPs in this network is five and they have high capacity and low cost, and this result is completely logical.

In the second scenario, the goal is that all power plant units are in the network, but the network load increases by 300 megawatts in total hours, and the performance of different power plant units is checked. In the second scenario, the goal is that all the power plant units are in the grid, but the grid load is increased by 300 megawatts and the performance of different power plant units is checked. This amount of load has increased in all hours. The production power of different power plant units for the second scenario is shown in Fig. 7.

As can be seen from Figure 7, the performance of the power plant units is similar to the previous scenario and the CHP units were able to meet all the load power. This issue is due to the low cost considered for this unit, and in order to definitively observe that the correct operation of the power plant units is carried out, the third scenario has been considered. In the third scenario, three important things have been done: 1- compared to the first scenario, the load has been halved, 2- The wind turbines in the first VPP have been taken off the grid due to technical problems, and 3- The CHP units in the third VPP were disconnected from the network from 1 am to 6 am due to technical reasons, and after solving the problems, they entered the network at 6 am.

In this scenario, the goal is that if the main unit of the

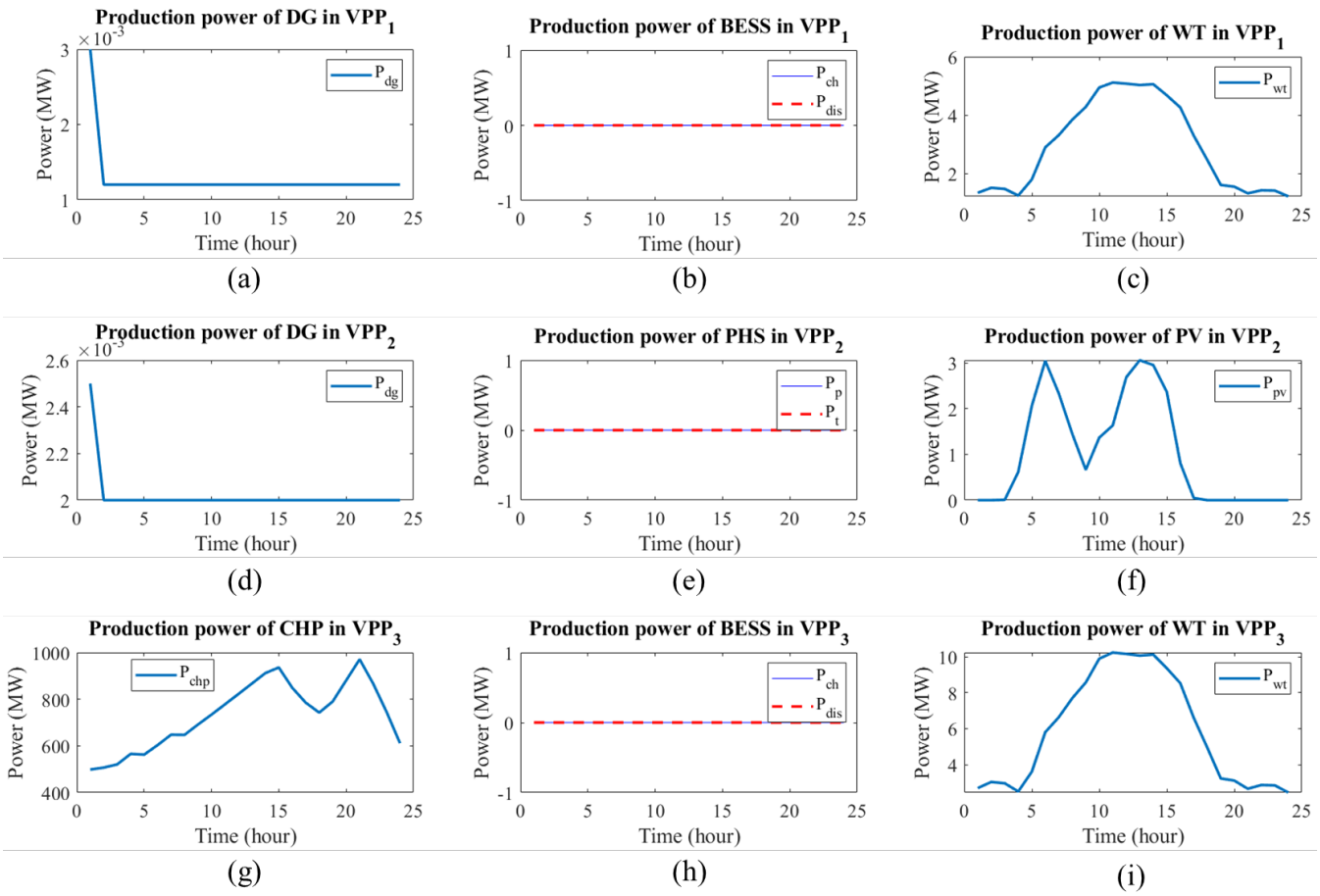


**Fig. 7. The power produced by different power plant units in the network (MW) in the scenario two. (a) Production power of DG in VPP1, (b) Production power of BEES in VPP1, (c) Production power of WT in VPP1, (d) Production power of DG in VPP2, (e) Production power of PHS in VPP2, (f) Production power of PV in VPP2, (g) Production power of CHP in VPP3, (h) Production power of BESS in VPP3, (i) Production power of WT in VPP3.**

network, which is CHP and has a large power generation capacity, cannot produce power in some hours, what will the rest of the power plant units do to prevent network outages. The result of power generation of power plant units in this network in the third scenario is shown in Fig. 8.

As can be seen from Figure 8, the production power in the first VPP wind turbines is absolutely zero, and this unit is off the grid. Also, based on subplot (g), in hours 1 to 6, CHP units in the third VPP are off the grid and do not generate power. To provide the power required by the load in hours 1 to 6, PHS units in the second VPP and BESS units in the first VPP have been added to the network and injected power into the network. Therefore, in this scenario, it was observed that if some units are removed from the network, the rest of the units are added to the network and take over power generation in order to balance the power in the network. In this scenario, the performance of energy storage units was observed and these units came to the aid of the grid in emergency situations. Similarly, different scenarios can be considered to make the problem as close to reality as possible.

One of the most important issues in the comparison between centralized and decentralized methods is the comparison of the solution time of the two methods. The duration of solving the modelled problem with the centralized method is 4.83 seconds, while with the decentralized ADMM algorithm, the solving time has reached 0.24 seconds. Based on this, the solution time for the decentralized method is about one-twentieth of the centralized method, and if the network becomes much larger, this issue will be much more important. It is expected that the use of decentralized methods in VPP networks will increase significantly.

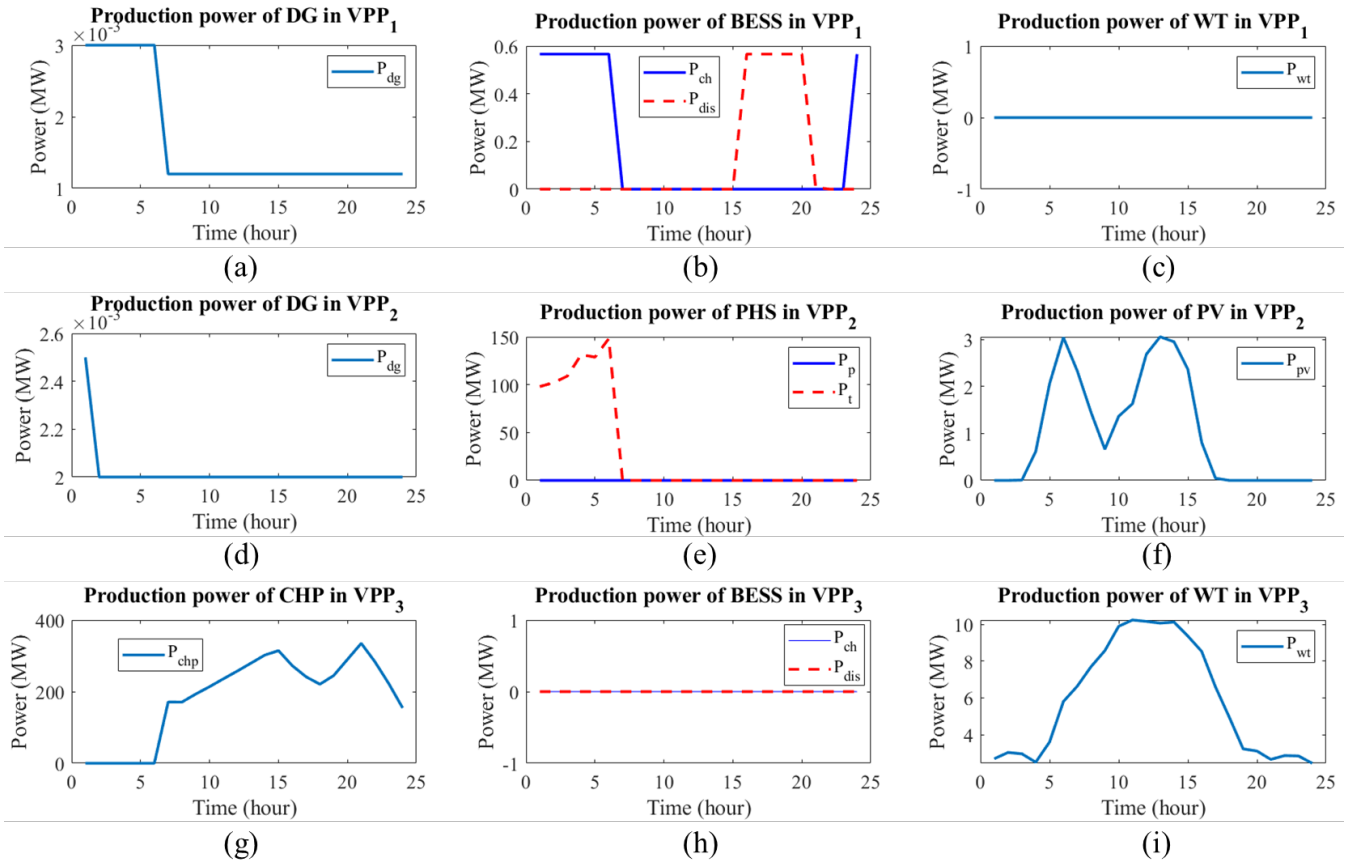


**Fig. 8. The power produced by different power plant units in the network (MW) in the scenario three. (a) Production power of DG in VPP1, (b) Production power of BEES in VPP1, (c) Production power of WT in VPP1, (d) Production power of DG in VPP2, (e) Production power of PHS in VPP2, (f) Production power of PV in VPP2, (g) Production power of CHP in VPP3, (h) Production power of BESS in VPP3, (i) Production power of WT in VPP3.**

## 5- Conclusion

Due to geographical expansion, the use of centralized optimization methods is limited for many reasons, including high computational load. To reduce the amount of computation, decentralized methods should be used. In this article, three virtual power plants are considered in the network, which, in addition to the limitations that exist on each power plant unit, must be able to respect the balance of electrical and thermal energy, on the one hand, to get maximum profit. A decentralized method was used to optimize them, and ADMM, Fast ADMM, and Fast ADMM with restart algorithm were used. Furthermore, the obtained results were compared with those obtained from the concentration method and similar results were obtained for them. In addition, the balance of electricity and heat has also been established in the network. The results obtained are acceptable and will increase the use of decentralized methods in the network of virtual power plants in the future. Finally, it was observed from the simulations that the solution time of decentralized algorithms is much lower than the centralized method and shows the application of these algorithms.

## References

[1] X. Dong, Y. Hua, Y. Zhou, Z. Ren, Y. Zhong, "Theory and experiment on formation-containment control of multiple multirotor unmanned aerial vehicle systems", IEEE Transactions on Automation Science and Engineering, 2018, 16(1), 229–240.

[2] W. Gao, J. Gao, K. Ozbay, Z. Jiang, "Reinforcement-learning-based cooperative adaptive cruise control

of buses in the Lincoln-tunnel corridor with time–varying topology". IEEE Transactions on Intelligent Transportation Systems, 2019.

[3] Z. Zhang, J. Du, K. Zhu, J. Guo, M. Li, T. Xu, "Optimization scheduling of virtual power plant with carbon capture and waste incineration considering P2G coordination", Energy Reports, 2022.

[4] Y. Wang, M. Zhang, J. Ao, Z. Wang, H. Dong, M. Zeng, "Profit Allocation Strategy of Virtual Power Plant Based on Multi-Objective Optimization in Electricity Market", sustainability, 2022.

[5] W. Chen, Y. Xiang, J. Liu, "Optimal operation of virtual power plants with shared energy storage", IET Smart Grid, 2022.

[6] A. Shahkoomahalli, A. Koochaki, and H. Shayanfar, "Two-stage Operational Planning of a Virtual Power Plant in the Presence of a Demand Response Program", Journal of Applied Dynamic Systems and Control, Vol.5, No.1, 2022.

[7] Y. Chen, Q. Du, M. Wu, L. Yang, H. Wang, and Z. Lin, "Two-stage optimal scheduling of virtual power plant with wind-photovoltaic-hydro-storage considering flexible load reserve", 2022 The 4th International Conference on Clean Energy and Electrical Systems (CEES 2022), 2–4 April, 2022.

[8] J. Cao, Y. Zheng, X. Han, D. Yang, J. Yu, N. Tomin, P. Dehghanian, "Two-stage optimization of a virtual power plant incorporating with demand response and energy complementation", Energy Reports 8, 2022.

[9] H. Wang, Y. Jia, C. S. Lai, K. Li, "Optimal Virtual Power Plant Operational Regime under Reserve Uncertainty", IEEE, 2022.

[10] H. Sharma, S. Mishra, "Optimization of Solar Grid-Based Virtual Power Plant Using Distributed Energy Resources Customer Adoption Model: A Case Study of Indian Power Sector", Arabian Journal for Science and Engineering, 2021.

[11] Z. Ullah, A. Arshad, H. Hassanin, "Modeling, Optimization, and Analysis of a Virtual Power Plant Demand Response Mechanism for the Internal Electricity Market Considering the Uncertainty of Renewable Energy Sources", energies, 2022.

[12] X. Wei, Y. Xu, H. Sun, H. Zhao, "Bi-level Hybrid Stochastic/Robust Optimization for Low-Carbon Virtual Power Plant Dispatch", CSEE Journal of Power and Energy Systems, 2021.

[13] Z. Ullah, A. Arshad, H. Hassanin, J. Cugley, M. A. Alawi, "Planning, Operation, and Design of Market-Based Virtual Power Plant Considering Uncertainty", energies, 2022.

[14] S. Maiz, L. Baringo, R. G. Bertrand, "Expansion planning of a price-maker virtual power plant in energy and reserve markets", Sustainable Energy, Grids and Networks, ELSEVIER, 2022.

[15] A. H. Gholami, A. A. Suratgar, M. B. Menhaj, M. R. Hesamzadeh, "Establishment of a Virtual Power Plant in Grid for Maximizing Producers' Profits and Minimizing Pollutant Emissions and Investment Costs", 30th International Conference on Electrical Engineering (ICEE), 2022.

[16] L. Yavuz, A. Önen, S. M. Muyeen, and I. Kamwa, "Transformation of microgrid to virtual power plant—A comprehensive review", IET Gener., Transmiss. Distrib., vol. 13, no. 11, pp. 1994–2005, Jun. 2019.

[17] B. Hu, H. Wang, T. Niu, C. Shao, C. Li, "Multi-time-scale coordinated optimal dispatch of virtual power plant under unreliable communication", CSEE Journal of Power and Energy Systems", pp. 1-10, 2021.

[18] W. Liu, H. Xu, X. Wang, S. Zhang, T. Hu, "Optimal dispatch strategy of virtual power plants using potential game theory", The 5th International Conference on Electrical Engineering and Green Energy, CEEGE, vol. 8, pp. 1069-1079, 2022

[19] W. Chen, Y. Xiang, J. Liu, "Optimal operation of virtual power plants with shared energy storage", IET Smart Grid, No. 24, 2022.

[20] H. Eisazadeh, M. M. Moghaddam, B. Alizadeh, "Optimal frequency response of VPP-based power systems considering participation coefficient", International Journal of Electrical Power and Energy Systems, ELSEVIER, vol. 129, 2021.

[21] A. Suratgar, M. B. Menhaj, Distributed Optimization and Its Application in Electricity Grids, Including Electrical Vehicle, Book chapter of "Electric Transportation Systems in Smart Power Grids: Integration, Aggregation, Ancillary Services, and Best Practices", Chapter 19, Taylor & Francis, 2023.

[22] SM Malakouti, MB Menhaj, AA Suratgar, The usage of 10-fold cross-validation and grid search to enhance ML methods performance in solar farm power generation prediction , Cleaner Engineering and Technology 15, 100664, 2023

[23] A. Saadati Moghadam, A. A. Suratgar, M. R. Hesamzadeh, S. K. Y. Nikravesh, A Distributed Approach for Solving AC-DC Multi-Objective OPF Problem, International Journal of Electrical Power & Energy Systems, Vol.153, 2023.

[24] Amir Hossein Gholami, Amirabolfazl Suratgar, Mohammad Bagher Menhaj, Mohammad Reza Hesamzadeh, Distributed and Decentralized Optimization with Unknown Agents: A Virtual Power Plant Scheduling Application, SSRN, 2023.

[25] Z. Goudarzi, J. Bagherinejad, M. Rafiee. A. A. Suratgar, Optimizing Investment of Pumped storage Systems for Renewable Energy Future, Journal of Optimization and Industrial Engineering, Vol.16. pp 167-184, 2023. DOI10.22094/JOIE.2023.1974939.2022

[26] B. Farzanegan, M.B. Menhaj, A. A. Suratgar, M. Zanmani, Distributed optimal control for continuous-

time nonaffine nonlinear interconnected systems, International Journal of Control, 95 (12), pp: 3462-3476, 2022.

[27] A. Saadati Moghadam, A. A. Suratgar, M. R. Hesamzadeh, S. K. Y. Nikravesh, Multi-objective ACOPF using distributed gradient dynamics, International Journal of Electrical Power & Energy Systems, Vol.141, 2022.

[28] S. Asgari, A. A. Suratgar, M. G. Kazemi, Feedforward fractional order PID load frequency control of microgrid using harmony search algorithm, Vol. 45, No.4, pp1369-1381,2021.

[29] S Asgari, MB Menhaj, AA Suratgar, MG Kazemi, A Disturbance Observer Based Fuzzy Feedforward Proportional Integral Load Frequency Control of Microgrids, International Journal of Engineering 34 (7), 1694-1702, 2021.

[30] E Ranjbar, MB Menhaj, AA Suratgar, J Andreu-Perez, M Prasad, Design of a fuzzy PID controller for a MEMS tunable capacitor for noise reduction in a voltage reference source, SN Applied Sciences, Springer International Publishing, Vol.3, pp:1-17, 2021.

[31] B. Farzanegan, M. Zamani, A.A. Suratgar, M.B. Menhaj, A neuro-observer-based optimal control for nonaffine nonlinear systems with control input saturations, Control Theory and Technology, vol19, no.2, 283-294, 2021 .

[32] Jafar Tavoosi, Amir Abolfazl Suratgar, Mohammad Bagher Menhaj, Amir Mosavi, Ardashir Mohammadzadeh, and Ehsan Ranjbar, Modeling Renewable Energy Systems by a Self-Evolving Nonlinear Consequent Part Recurrent Type-2 Fuzzy System for Power Prediction, Sustainability, Vol.13, no.6 , pp:1-21, 2021.

[33] S. Hashempour, A. A. Suratgar, A.Afshar, Distributed Non-Convex Optimization for Energy Efficiency in Mobile Ad-Hoc Networks, IEEE System Journals, Vol.15, no.4, pp:5683-5693, 2021.

[34] O. P. Akkas, E. Cam, " Optimal operational scheduling of a virtual power plant participating in day-ahead market with consideration of emission and battery degradation cost", International Transaction Electric Engineering System, 2020.

[35] Z. Jing, J. Zhu, R. Hu, "Sizing optimization for island microgrid with pumped storage system considering demand response", MPCE (J. Mod. Power Syst. Clean Energy), 2017.

[36] R. Nishihara, L. Lessard, B. Recht, A. Packard, M. I. Jordan, "A General Analysis of the Convergence of ADMM", 32 nd International Conference on Machine Learning, 2015.

[37] T. Goldstein, B. O. Donoghue, S. Setzer, R. Baraniuk, "Fast Alternating Direction Optimization Methods", Industrial and Applied Mathematics, SIAM, 2014.

[38] M. Shivaie, M. Mokhayeri, M. K. Moghaddam, A. Ashouri-Zadeh, "A reliability-constrained cost-effective model for optimal sizing of an autonomous hybrid solar/wind/diesel/battery energy system by a modified discrete bat search algorithm", Solar Energy, pp. 344-356, 2019.

[39] B. M. Ivatloo, M. M. Dalvand, A. Rabiee, "Combined heat and power economic dispatch problem solution using particle swarm optimization with time varying acceleration coefficients", Electric Power Systems Research, pp. 9-18, 2013.

**HOW TO CITE THIS ARTICLE**

*A. H. Gholami, A. A. Suratgar, M. B. Menhaj, M. R. Hesamzadeh, Decentralized Optimization in the Scheduling of Three Virtual Power Plants with Non-Convex Constraints, AUT J. Model. Simul., 56(1) (2024) 3-18.*

**DOI:** 10.22060/miscj.2024.23304.5364